*Metrol. Meas. Syst.*, Vol. 26 (2019) No. 1, pp. 153–169.

PAN POLSKA AKADEMIA NAUK

METROLOGY AND MEASUREMENT SYSTEMS

Index 330930, ISSN 0860-8229

*www.metrology.pg.gda.pl*

M&MS

# CHARACTERIZATION OF MULTI-EMITTER TUNEABLE LED SOURCE FOR ENDOSCOPIC APPLICATIONS

**Urszula J. Błaszczak, Łukasz Gryko, Andrzej S. Zając**

*Bialystok University of Technology, Faculty of Electrical Engineering, 15-351 Białystok, Wiejska 45D, Poland*
(✉ *u.blaszczak@pb.edu.pl*, +48 85 746 9447, *l.gryko@pb.edu.pl*, *andrzej.zajac@wat.edu.pl*)

**Abstract**

In this paper we describe our own construction of a tuneable light source based on a set of light emitting diodes covering the visible spectrum using a homogenizing rod instead commonly used low energy-efficient integrating spheres. The expected prime application of the source is a medical endoscopic system, however it is possible to use it also for other purposes requiring both multispectral operation and a tuneable white light source. We describe the construction of the source and include precise characterization of the output white light – distribution of CCT, $Duv$, $\Delta u'v'$ and colour rendering indexes ($R_a$, $R_9$, $R_f$, $R_g$) of light in several planes located at various distances. The obtained results prove that our source is characterized by very good colour rendition according to the $R_a$ and $R_f$ method for various correlated colour temperatures (2700–6500) K. As an example of application images of the Macbeth colour chart registered with an RGB camera included in the laboratory measurement stand are presented. The obtained results prove that, after whole system calibration, this source can be used in many applications, where evaluation of objects requires precise analysis of their colour and multispectral procedures.

Keywords: measurement, medical applications, LED, tuneable source.



## 1. Introduction

Humans have evolved under natural light. For this reason our eyes and the way we recognize and analyse objects are strongly dependent on the lighting conditions. Several areas of science give us a possibility to learn and deepen our knowledge on how our visual system works. Understanding its operation is still not complete, but we know that continuous changes of *spectral power distribution* (SPD) of natural light has many consequences to the way of functioning of humans. By changing the spectra of light used to illuminate objects we may – intentionally or not – control their visibility or their selected features.

Lamps that spectrally follow the natural light (daylight) have been used for many years, however constructions of such lamps were restricted by limited possibilities of mixing gases filling the discharge lamps. Development of *light emitting diodes* (LEDs) has rapidly increased the number of applications of these light sources in various areas of engineering, also for simulation of daylight. *Phosphor-converted LEDs* (PC LEDs) emitting white light are widely used for general illumination and all applications where white light is necessary. Their main advantages

Article history: received on Sep. 06, 2018; accepted on Nov. 07, 2018; available online on Mar. 29, 2019, DOI: 10.24425/mms.2019.126332.

are widely known: high energy efficiency when compared with traditional light sources, but also higher flexibility in adjusting output parameters of lighting systems (including SPD adjustment), reduced size, robustness and absence of unnecessary ranges of radiation (ultraviolet and infrared). Nowadays, when LED chips are available from the UV, through visible and up to infrared range of the electromagnetic spectra, a variety of applications of LEDs [1] are obvious.

LEDs emitting white light have successfully substituted traditional sources also in endoscopic applications [2–6], however many research results prove that PC LEDs tend to limit visual performance due to their spectral power distribution shape [7]. It was also proved that better colour rendering assures better vision without increasing amount of light [8], however for many years it has been known that PC LEDs do not assure high rendering of colours [7, 9], especially in the long wave part of visible spectrum. For this reason multi-emitter tuneable LED sources has been researched in lighting technology for over decade [10, 11]. Various algorithms for selecting chips were proposed so that the entire spectral match could be obtained for various phases of daylight [12–14]. Tuneable sources have been used in various applications recently, for example in general lighting [15–18], as this solution gives better performance in terms of colour recognition in interiors, but also enables to influence the circadian rhythm through control of the melatonin level [19]. LEDs are also being substituted for traditional lamps in support of plant growth [18, 20]. Traditionally, red and blue light-emitting chips are used as they are recognized to be the most efficient, however new research on and applications with more complex spectra appear. In a wide range of research and industrial applications multi-emitter LED systems are used to improve quality control and information mining [21–24]. Complex LED-based lighting systems are also being designed for medical applications in the UV, VIS and IR ranges [25–30]: fluorescence microscopy, phase imaging of human cells, detection of skin, tissue and cell dysfunctions by analysis of spectral images. In this paper we present our own construction of a tuneable LED-based source which intentionally is dedicated to endoscopic applications [31].

## 2. Construction of source

The general purpose of this research was to construct a source that would be used in endoscopic systems, where light is provided to the region of interest by optical fibres and is the only source of light. For uniform (in a spectral sense) illumination of the tissue, when a single source is used, the construction is simple and the major problem is to assure its high coupling efficiency. Typically, PC LEDs are nowadays used in endoscopes, however the problem of poor colour rendition of this kind of source is known, especially when wavelengths from the red region are taken into account [7]. The solution for this problem is to use a multi-emitter system, where the SPD of PC LED is filled with monochromatic emitters to obtain white light of high quality.

In general lighting the SPD of white light can be characterized by several parameters, for example: a *correlated colour temperature* (CCT), a distance and direction of a colour shift from the Planckian locus on either CIE 1960 $u-v(Duv)$ or CIE 1976 $u'-v'(\Delta u'v')$ coordinate system, a general colour rendering index ($R_a$) and specific indexes ($R_1-R_{14}$), a colour fidelity index $R_f$ a Gamut index $R_g$ [32]. All these parameters (their distribution) were measured on planes at different distances from the output of the source. These parameters are based on the results of many years of research in terms of correct recognition of objects illuminated by various SPDs, thus some of them – also these associated with colour recognition – are frequently taken into account as the criteria for the spectral composition of multi-emitter sources [33]. In this kind of application however, an additional criterion usually means different SPD, which is also affected

by an assumed amount of spectral components and for this reason we can observe a variety of possible technical solutions [34–37].

A general colour rendering index ($R_a$) describes how well–on average – a set of test colour samples is reproduced under characterized illumination when compared with reference spectra of the same colour temperature (illuminant). In this method a set of 8 colour samples with 6 additional ones is used. The maximum value of the index is 100 and a difference of at least 5 is recognized by humans. In general lighting the value of 80 is recognized as good. However, in medical applications more strict requirements are set including the condition for a very high value of $R_9$ index, which is not included in calculation of $R_a$. Although International Commission of Illumination suggests to use a colour fidelity index ($R_f$) in scientific applications [38], especially for characterization of PC-LEDs, no requirements are given to define expected values of each component of this index in various applications. Also a Gamut index still has no border quality values – $R_g = 100$ means that a light source has no differences in relation to the illuminant in chroma or saturation of the same set of samples as in the $R_f$ method. Values lower than 100 appear when the light source on average renders samples as less saturated, while higher than 100 – when it is more saturated than the reference source. For this reason we assumed that our system should provide $R_a$ and a specific colour rendering index $R_9$ not lower than 92 [39]. Achieving these values was one of the criteria during selection of components for our multi-emitter system from the ones available on the market. The second criterion was applicability of radiation of the components in *photodynamic therapy* (PDT) [40]. To select the components of the source we made simulations [41] and chose a set of 13 LEDs including 11 monochromatic and 2 phosphor-converting emitters (Fig. 1) [42]. They were characterized electrically and spectrally [42], which let us use the real characteristics of each emitter to design and develop a control system providing capability of changing the correlated colour temperature of the output white light and quasi-monochromatic light [43, 44].

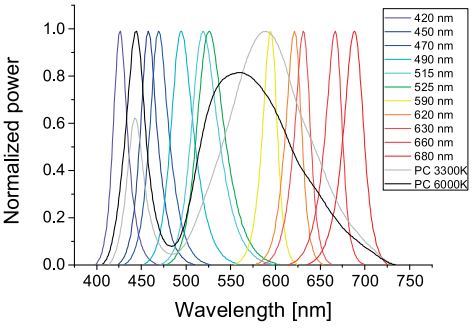


Fig. 1. Relative spectral power distributions of LED components of the source; LEDs were power-supplied with a maximum current.

However, this idea generated a new problem of delivering a stable and uniform beam from each LED to the tissue area. It is not possible to couple each source directly with the illuminating fibres as it would not assure uniform illumination of the tissue (in a sense "the same or very similar spectral distribution of light in each point of the illuminated object") and satisfying colour homogenizing, also because of a short working distance of the endoscopic head. For white LED-based endoscopes this problem does not exist. For this reason the construction of the source has to include an SPD's homogenizing element. The best method to obtain a uniform spectral characteristic for a multi-emitter source is to use an integrating sphere that assures uniformity

of luminance and SPD at its exit window. However, the price of integrating spheres and their low efficacy are their disadvantages. Additionally, their output power decreases significantly with the increase of their diameters. For this reason we used a homogenizing rod (Fig. 2). Light from the set of LEDs is provided by 3 mm *plastic optical fibres* (POF) to a rectangular-shaped *homogenizing rod* (HR) (cross-section 20 mm × 19 mm, length $L$ = 200 mm) [14, 45, 46]. At the output surface of the rod a diffuser (N-BK7 Ground Glass Diffuser, 120 Grit) is used, which improves the uniformity of light emitted from HR. This plane is the output plane of the source, that can be coupled with the branch of optical fibres or used in another application requiring monochromatic radiation or high-quality white light of different CCT. With this technique we control the spectral composition of light in each illuminating fibre and we can change these spectra depending on the requirements within an assumed range.

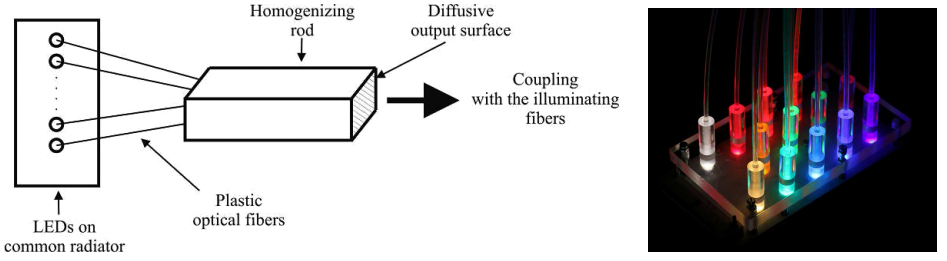


Fig. 2. A scheme of the source (left) and a view of LEDs-plastic optical fibres coupling (right).

As the coupling efficiency of each LED with an optical fibre providing light to the homogenizing rod can be different, we have performed measurements of total optical power at the output of each coupling fibre, which enabled to simulate the operation of the homogenizing rod [45, 46], select the supply for each component for each assumed spectral distribution of the output white light beam (illuminant A – 2856 K, 3500 K, 4500 K, D55 and D65) [45] and characterize its quality according to CIE colorimetric parameters [7, 38]. SPDs of output white light for each CCT were measured at 6 distances from the output of the optical homogenizing rod – 5, 10, 15, 20, 25, 30 mm (examples in Fig. 3).

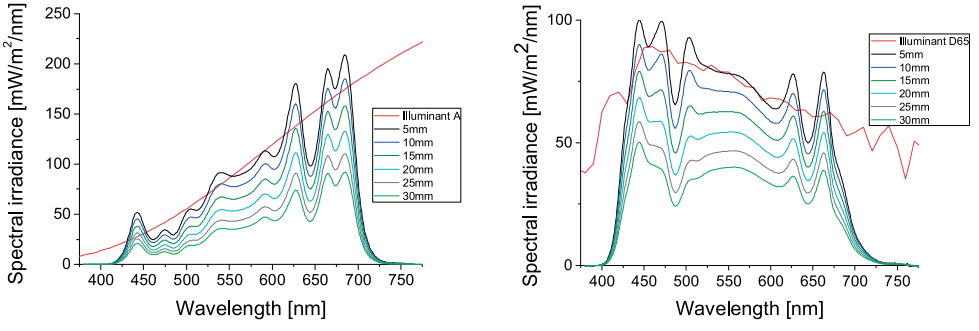


Fig. 3. Examples of measured output SPDs (white light) at 2856 K (left), at 6500 K (right).

The power consumed by the whole system was 11.5 W. The maximum density of optical radiation at the output (the surface of the diffuser) was about 15 mW/cm$^2$. The energy efficiency of this source is not high as it was optimized from a point of view of other parameters.

### *2.1. Characterization of source*

In order to characterize the constructed light source we carried out measurements that let us understand the operation of this system in terms of spatial uniformity of output radiation defined as similarity of spectra and colorimetric parameters in different areas of the output beam. The measurements were taken on the stand presented in Fig. 4. LEDs were mounted on the cooling radiator with its thermal resistance lower than necessary. It assures stable operation conditions of LEDs. For each of them the current was set independently. All elements of the stand were mounted on the optical bench to ensure stability during the procedure. For measurements we used a calibrated spectrometer GL Spectis Touch 1.0 (the radiometric and photometric calibration uncertainty < 4%) in two configurations: first – the spectrometer with the diffuser for measurements of average SPD on selected planes and second – the spectrometer with the diffuser and a 1 mm diameter diaphragm for measurements of SPDs' distribution on selected planes (the uniform measuring grid 5 × 5 points). The meter was mounted on the 3-axis stage enabling to move it along and crosswise the optical axis.

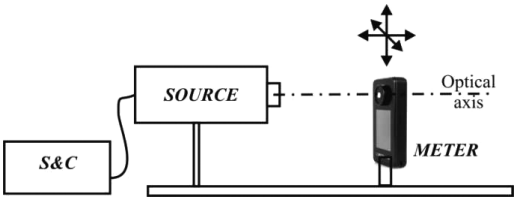


Fig. 4. A scheme of the measurement stand (S&C – supply and control system of the source; the meter with an optional diaphragm).

The aim of measurements was to examine the CCT and selected colorimetric parameters of the output white light beam. For characterization along the optical axis we measured the averaged value of spectral distribution (according to a cosine function of the diffusive cap of the spectrometer) for each assumed CCT composition (warm white-based and cool white-based) at 6 distances (5, 10, 15, 20, 25 and 30 mm) from the output surface of the source by moving the meter along the optical bench. In general, increasing the distance from the output surface causes a decrease of average CCT of the beam (Fig. 5).

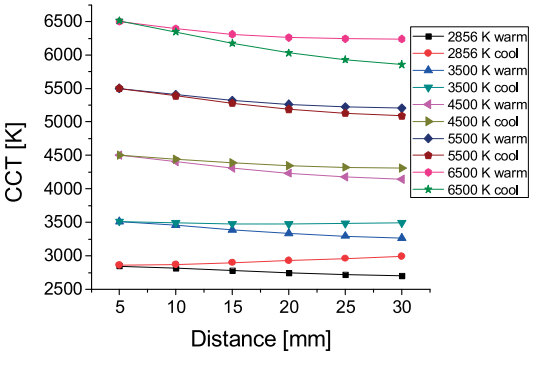


Fig. 5. Average correlated colour temperature CCTs of the source for selected SPDs along the optical axis.

For the lowest CCTs (2856 K and 3500 K) the changes are less significant, but also ΔCCT tolerance is lower (Table 1). In one exceptional case – for 2856 K tuned on the basis of cool white LED – we observed an increase of the CCT. The highest difference occurred between measurements for 5 mm and 30 mm distances, however in one case (3500 K tuned on the basis of cool PC LED) it occurred between 5 mm and 20 mm. In most cases ΔCCT of the source is within the tolerance for solid-state lighting (Table 1). Three compositions: 4500 K warm white-based, 5500 K cool white-based and 6500 K cool white-based did not meet the requirements that were exceeded by 120 K, 80 K and 150 K, respectively.

Table 1. Specifications of the correlated colour temperatures for solid-state lighting [29].

| **Nominal CCT [K]** | 2700 | 3000 | 3500 | 4000 | 4500 | 5000 | 5700 | 6500 |
|---|---|---|---|---|---|---|---|---|
| **Target CCT and its tolerance ΔCCT [K]** | 2725 ±145 | 3045 ±175 | 3465 ±245 | 3985 ±275 | 4503 ±243 | 5029 ±283 | 5667 ±355 | 6532 ±510 |

From a point of view of quality of white light the information about CCT of the light is insufficient as many spectra may be characterized by the same CCT. For this reason other quantities are used, like coordinates in the chromaticity diagram that enable to calculate other quality parameters. Location of each tuned white light in the $u'v'$ chromaticity diagram (Fig. 6) proves that although the spectra are changing along the optical axis, the changes are not significant. For each assumed CCT we can observe at least one case with high colorimetric stability of output light that stays within the range accepted by the standards for LEDs emitting white light [32] – the chromatic coordinates of light stay inside 7-step MacAdam ellipses and for 2856, 3500 and 4500 K inside 4-step MacAdam ellipses.

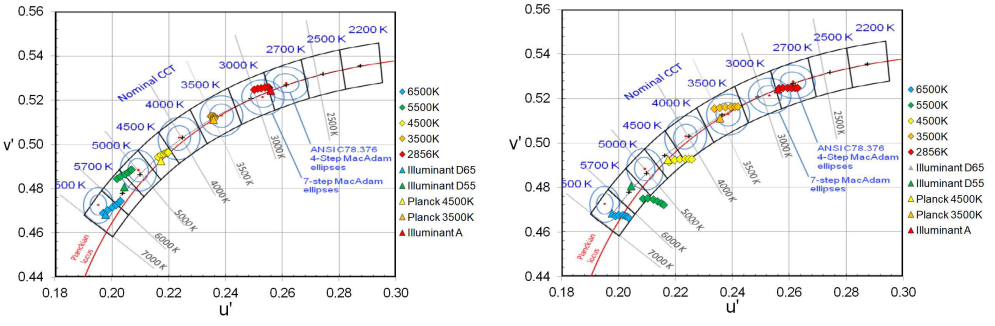


Fig. 6. Chromaticity diagrams for assumed CCTs: cool white-based (left) and warm white-based (right) along the optical axis (distances measured from the output surface of the source from 5 mm to 30 mm with step 5 mm).

To characterize quality of the obtained white light, on the basis of measured spectra we calculated selected colorimetric parameters: the distance from the reference point (usually on the Planckian locus) *Duv*, the general colour rendering index $R_a$ and the specific colour rendering index $R_9$. The results of calculation are presented in Figs. 7 and 8.

The results show that in terms of the general colour rendering index our source is characterized by smaller variations with distance, thus is more stable for spectra tuned with a warm white LED. Additionally, for cool white-based spectra we observed a more significant decrease of $R_9$ index with distance.

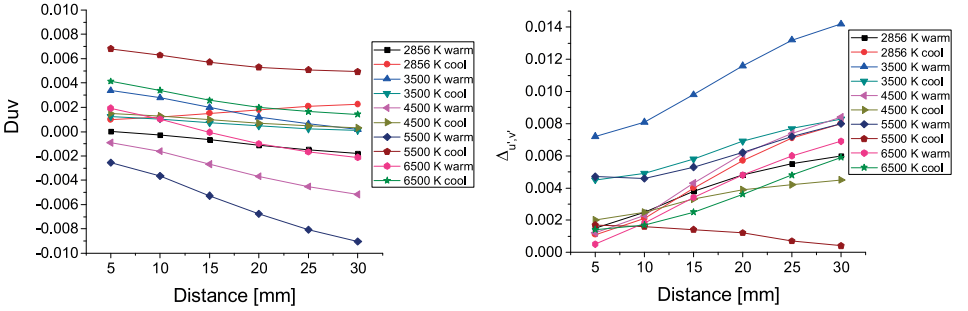


Fig. 7. Colour shift *Duv* of the source for assumed CCTs: cool and warm white-based along the optical axis (distances measured from the output surface of the source) (left); $\Delta u'v'$ of the source for assumed CCTs: cool white- and warm white-based along the optical axis (distances measured from the output surface of the source) (right).

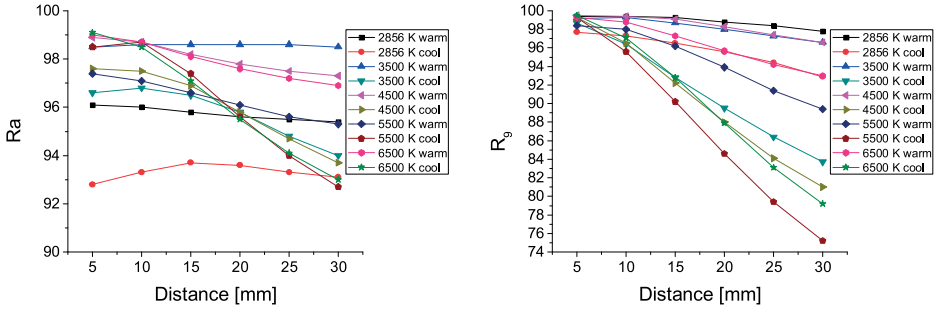


Fig. 8. Rendering index $R_a$ of the source for assumed CCTs: cool and warm white-based along the optical axis (distances measured from the output surface of the source) (left); $R_9$ of the source for assumed CCTs: cool and warm white-based along the optical axis (distances measured from the output surface of the source) (right).

We have also analysed the value of colour fidelity index $R_f$ (Fig. 9), which is suggested for the scientific use when characterization of white light quality is included [38].

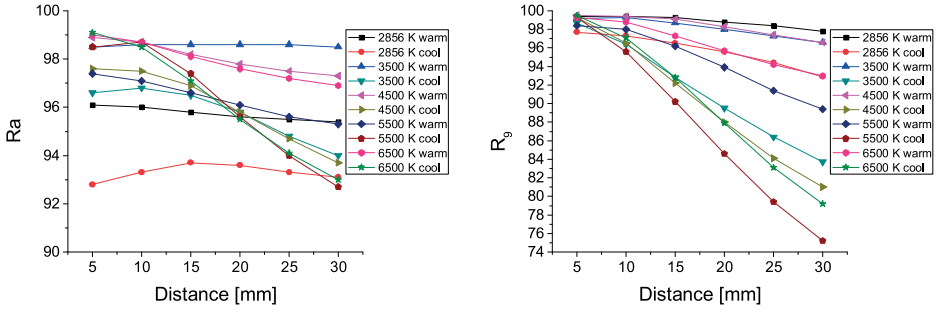


Fig. 9. Rendering indexes $R_f$ (left) and $R_g$ (right) of the source for assumed CCTs: cool and warm white-based along the optical axis (distances measured from the output surface of the source).

According to the results the general colour fidelity index and the Gamut index of our source stay respectively: between 89 and 99 and between 98 and 106 with changes of distance. It suggests very good rendering of 99 colour samples, however according to these methods there are no border values for various applications. The Gamut index specifying how full or saturated is the spectrum

(that is why the $R_g$ value can be above 100, since it can give more saturated images than normal light).

According to the performance standards of LED [32] sources the target tolerance of $Duv$ is ±0.006. The colour shift $\Delta u'v'$ can be derived from MacAdam ellipses (they are not standardized) – for a 7-step ellipse it is 0.0077. Both parameters were calculated for each LED-based source with reference to illuminants A, D55, D65 and perfect black body of 3500 K and 4500 K.

Analysis of our results (Table 2) proves that for each assumed CCT at least one version (bold in Table 2) of tuned spectra of our source is characterized by better colorimetric properties than required. In fact only for the D55 spectra ($Duv$ = 0.0068) the performance standard is exceeded. This colorimetric effect was obtained by complementing the spectra of white-light emitting diode with light emitted by narrow-band diodes of different colours. As a result we obtained a source with better colour rendering than the most popular sources – PC LEDs [7] and fluorescent lamps. The difference is significant, especially for $R_9$ index, which is usually below 40 for these sources [7]. The results of measurements and analysis prove that after illuminating objects with our source their colour expressed by $R_a$ should be recognized correctly for each tuned CCT.

Table 2. Comparison of maximum differences of CCT and maximum values of chromaticity parameters $Duv$ and $\Delta u'v'$ for each CCT, when changing distance along the optical axis.

| CCT [K] | Warm white based | | | Cool white based | | |
|---|---|---|---|---|---|---|
| | \|ΔCCT max\| [K] | \|(*Duv*)max\| | \|(Δ*u′v′*)max\| | \|ΔCCT max\| [K] | \|(*Duv*)max\| | \|(Δ*u′v′*)max\| |
| 2856 | **144** | **0.0018** | **0.0060** | **129** | **0.0022** | **0.0080** |
| 3500 | 247 | 0.0034 | 0.0142 | **35** | **0.0012** | **0.0083** |
| 4500 | 366 | 0.0052 | 0.0084 | **195** | **0.0015** | **0.0045** |
| D55 | 295 | 0.0091 | 0.0080 | 412 | 0.0068 | 0.0017 |
| D65 | **263** | **0.0021** | **0.0069** | 656 | 0.0041 | 0.0059 |

For each CCT we also measured SPDs of the output light in cross-section in several distances to determine uniformity of parameters of the output beam. An additional diaphragm (1 mm diameter) was mounted on the input of the meter (the diffusive cap of the spectrometer GL Spectis Touch 1.0) in order to limit its field of view. The measurement grid was uniform 5 × 5 points. Below in Tables 3–7 we present selected results – for extreme planes (distant by 5 mm

Table 3. Colorimetric and photometric parameters in 25 points of 2856 K warm-based white light at distances of 5 and 30 mm from the output surface of the source.

| **Distance [mm]** | **5** | | | | | | | | **30** | | | | | | | |
|---|---|---|---|---|---|---|---|---|---|---|---|---|---|---|---|---|
| **quantity** | **CCT [K]** | ***Duv*** | **Δ*u′v′*** | ***Ra*** | ***R*9** | ***Rf*** | ***Rg*** | **illuminance [lx]** | **CCT [K]** | ***Duv*** | **Δ*u′v′*** | ***Ra*** | ***R*9** | ***Rf*** | ***Rg*** | **illuminance [lx]** |
| **minimum** | 2673 | −0.0010 | 0.0021 | 95 | 83 | 94 | 103 | 30 | 2622 | −0.0018 | 0.0032 | 95 | 84 | 93 | 104 | 22 |
| **maximum** | 2843 | 0.0015 | 0.0083 | 96 | 95 | 95 | 105 | 102 | 2788 | 0.0004 | 0.0107 | 96 | 91 | 95 | 106 | 43 |
| **Δ** | 170 | 0.0025 | 0.0062 | 1 | 12 | 1 | 2 | 72 | 166 | 0.0022 | 0.0074 | 1 | 7 | 2 | 2 | 21 |
| **medium** | 2747 | 0.0005 | 0.0051 | 95 | 89 | 95 | 104 | 77 | 2677 | 0.0011 | 0.0081 | 95 | 88 | 93 | 105 | 34 |
| **Uniformity of illuminance** | | | | | | | | 0.39 | | | | | | | | 0.65 |

Δ – difference between maximum and minimum values of parameter

uniformity = minimum/medium

and 30 mm from the output of the source) on a square area with 20 mm side length for each tuned CCT. We also calculated uniformity of illuminance of the object at each distance according to the definition accepted in general lighting. We observe better uniformity for higher CCT of output light.

Table 4. Colorimetric and photometric parameters in 25 points of 3500 K cool-based white light at distances of 5 and 30 mm from the output surface of the source.

| **Distance [mm]** | **5** | | | | | | | | **30** | | | | | | | |
|---|---|---|---|---|---|---|---|---|---|---|---|---|---|---|---|---|
| **quantity** | **CCT [K]** | ***Duv*** | **$\Delta u'v'$** | ***Ra*** | ***R*$_9$** | ***Rf*** | ***Rg*** | **illuminance [lx]** | **CCT [K]** | ***Duv*** | **$\Delta u'v'$** | ***Ra*** | ***R*$_9$** | ***Rf*** | ***Rg*** | **illuminance [lx]** |
| **minimum** | 3493 | 0.0018 | 0.0025 | 95 | 95 | 94 | 102 | 52 | 3484 | 0.0014 | 0.0020 | 94 | 94 | 92 | 102 | 34 |
| **maximum** | 3557 | 0.0045 | 0.0060 | 96 | 100 | 96 | 103 | 152 | 3532 | 0.0036 | 0.0049 | 96 | 99 | 95 | 103 | 73 |
| **Δ** | 64 | 0.0026 | 0.0035 | 1 | 5 | 2 | 1 | 100 | 48 | 0.0022 | 0.0030 | 2 | 5 | 3 | 1 | 39 |
| **medium** | 3516 | 0.0030 | 0.0041 | 96 | 98 | 95 | 102 | 120 | 3507 | 0.0021 | 0.0030 | 95 | 97 | 93 | 103 | 56 |
| **Uniformity of illuminance** | | | | | | | | 0.43 | | | | | | | | 0.61 |

Table 5. Colorimetric and photometric parameters in 25 points of 4500 K cool-based white light at distances of 5 and 30 mm from the output surface of the source.

| **Distance [mm]** | **5** | | | | | | | | **30** | | | | | | | |
|---|---|---|---|---|---|---|---|---|---|---|---|---|---|---|---|---|
| **quantity** | **CCT [K]** | ***Duv*** | **$\Delta u'v'$** | ***Ra*** | ***R*$_9$** | ***Rf*** | ***Rg*** | **illuminance [lx]** | **CCT [K]** | ***Duv*** | **$\Delta u'v'$** | ***Ra*** | ***R*$_9$** | ***Rf*** | ***Rg*** | **illuminance [lx]** |
| **minimum** | 4209 | 0.0021 | 0.0079 | 96 | 92 | 94 | 99 | 57 | 4165 | 0.0018 | 0.0082 | 94 | 86 | 92 | 99 | 37 |
| **maximum** | 4270 | 0.0049 | 0.0101 | 98 | 99 | 94 | 100 | 185 | 4249 | 0.0041 | 0.0096 | 98 | 99 | 94 | 101 | 91 |
| **Δ** | 61 | 0.0028 | 0.0023 | 2 | 7 | 1 | 1 | 128 | 84 | 0.0022 | 0.0015 | 4 | 13 | 2 | 2 | 53 |
| **medium** | 4230 | 0.0033 | 0.0089 | 97 | 97 | 94 | 100 | 144 | 4193 | 0.0025 | 0.0090 | 95 | 91 | 93 | 100 | 69 |
| **Uniformity of illuminance** | | | | | | | | 0.40 | | | | | | | | 0.54 |

Table 6. Colorimetric and photometric parameters in 25 points of D55 cool-based white light at distances of 5 and 30 mm from the output surface of the source.

| **Distance [mm]** | **5** | | | | | | | | **30** | | | | | | | |
|---|---|---|---|---|---|---|---|---|---|---|---|---|---|---|---|---|
| **quantity** | **CCT [K]** | ***Duv*** | **$\Delta u'v'$** | ***Ra*** | ***R*$_9$** | ***Rf*** | ***Rg*** | **illuminance [lx]** | **CCT [K]** | ***Duv*** | **$\Delta u'v'$** | ***Ra*** | ***R*$_9$** | ***Rf*** | ***Rg*** | **illuminance [lx]** |
| **minimum** | 5150 | 0.0056 | 0.0062 | 95 | 86 | 94 | 99 | 63 | 5004 | 0.0054 | 0.0079 | 92 | 78 | 92 | 99 | 33 |
| **maximumm** | 5324 | 0.0076 | 0.0085 | 99 | 99 | 96 | 99 | 141 | 5170 | 0.0070 | 0.0104 | 97 | 94 | 95 | 99 | 67 |
| **Δ** | 174 | 0.0020 | 0.0022 | 4 | 13 | 2 | 1 | 78 | 166 | 0.0017 | 0.0026 | 5 | 16 | 3 | 1 | 34 |
| **medium** | 5232 | 0.0066 | 0.0075 | 97 | 95 | 95 | 99 | 112 | 5071 | 0.0058 | 0.0094 | 94 | 84 | 93 | 99 | 51 |

In Fig. 10 the measurement results and distributions of the $u' - v'$ coordinates of the output light in two border cross-sections of the beam are presented.

Table 7. Colorimetric and photometric parameters in 25 points of D65 cool-based white light at distances of 5 and 30 mm from the output surface of the source.

| **Distance [mm]** | **5** | | | | | | | | **30** | | | | | | | |
|---|---|---|---|---|---|---|---|---|---|---|---|---|---|---|---|---|
| **quantity** | **CCT [K]** | ***Duv*** | **$\Delta u'v'$** | ***Ra*** | ***R*$_9$** | ***Rf*** | ***Rg*** | **illuminance [lx]** | **CCT [K]** | ***Duv*** | **$\Delta u'v'$** | ***Ra*** | ***R*$_9$** | ***Rf*** | ***Rg*** | **illuminance [lx]** |
| **minimum** | 6036 | 0.0019 | 0.0015 | 95 | 90 | 93 | 100 | 78 | 5917 | 0.0012 | 0.0019 | 95 | 87 | 93 | 100 | 38 |
| **maximum** | 6438 | 0.0041 | 0.0057 | 99 | 100 | 96 | 100 | 175 | 6354 | 0.0033 | 0.0072 | 99 | 100 | 96 | 101 | 81 |
| **Δ** | 402 | 0.0022 | 0.0042 | 4 | 10 | 3 | 1 | 97 | 437 | 0.0021 | 0.0053 | 4 | 13 | 3 | 1 | 43 |
| **medium** | 6237 | 0.0032 | 0.0035 | 98 | 95 | 95 | 100 | 138 | 6069 | 0.0017 | 0.0052 | 97 | 96 | 94 | 101 | 62 |

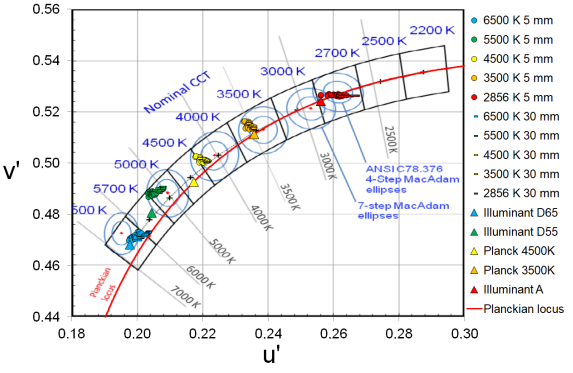


Fig. 10. A chromaticity diagram for 25 points of CCT 2856, 3500, 4500, 5500 and 6500 K cool-based and warm-based white light at 5 mm and 30 mm from the output surface of the source.

Changes of CCT for all sources in two planes are comparable, but medium CCTs for a 5 mm distance from the output of the source are lower (except 3500 K source) than those measured without a diaphragm. As a result, for larger distances we obtained CCTs not corresponding to the ranges from rectangular tolerance fields for solid-light sources, however the regularity of this phenomenon suggests that this may be influenced by the presence of the diaphragm in the measurement stand (the meter was calibrated for half-space).

In Figs. 11–13 we present distributions of CCT, $\Delta u'v'$ and $R_9$ in two planes (distant by 5 mm and 30 mm from the output of the source) for one SPD – cool white-based 4500 K. The graphs confirm stability of CCT, high quality of white light and its high colour rendering indexes.

The value of general colour rendering index $R_a$ is not worse than 94 (only for 5500 K and a distance of 30 mm – 92), and its variation stays below 5. The medium $R_9$ index value on both planes is not lower than 94. The medium value of $R_9$ index value (calculated on the surface at each distance) is not lower than 88, only for 5500K based on cool white-light emitting LED and a distance of 30 mm is 84. When we analyse the $R_9$ distribution on each surface, the lowest value is usually not below 83 with its detected minimum of 78. We also obtained very good results for $R_f$ index – in each point its value was not lower than 92 and variations were not bigger than 3 units. The average $R_f$ index value on each plane was not lower than 93. The value of Gamut index $R_g$ that describes the difference between the analysed spectra and the reference stays between 99 and 106 (the value 100 means the exact copy of the reference spectra).

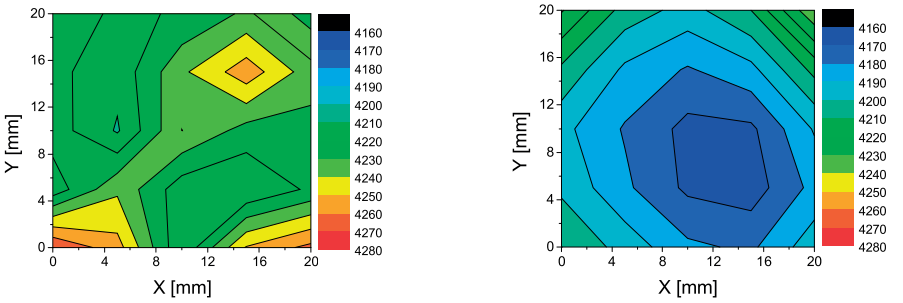


Fig. 11. A CCT distribution for 4500 K cool-based white light at 5 mm (left) and 30 mm (right) distances from the output surface of the source (X, Y – coordinates of the measurement points on the plane).

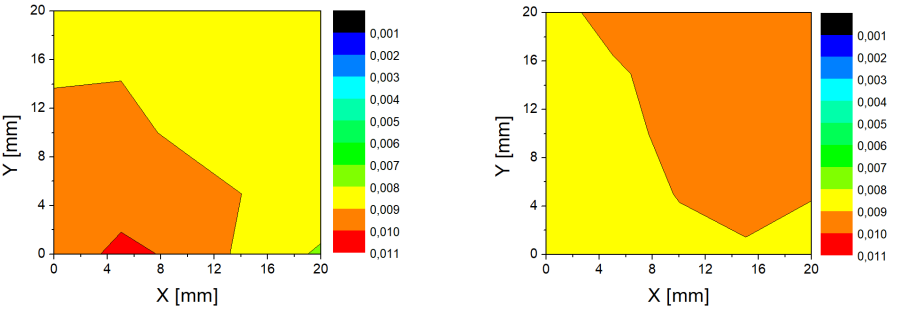


Fig. 12. A colour shift $\Delta u'v'$ distribution of 4500 K cool-based white light at 5 mm (left) and 30 mm (right) distances from the output surface of the source (X, Y – coordinates of the measurement points on the plane).

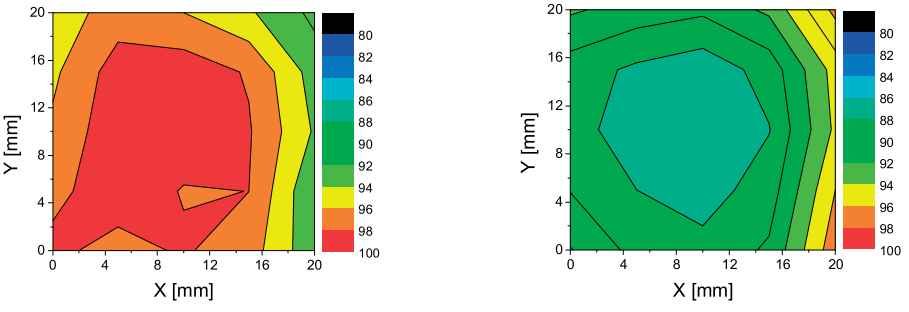


Fig. 13. A rendering index $R_9$ distribution of 4500 K cool-based white light at 5 mm (left) and 30 mm (right) distances from the output surface of the source (X, Y – coordinates of the measurement points on the plane).

## 3. Examples of measurement results

To test our source in practice we used it for tuneable and multispectral illumination of an object, which was then registered with an RGB micro-camera. An example of typical shapes of spectral sensitivity curves of RGB camera is presented in Fig. 14. For the experiment we chose the RGB Adobe Macbeth colour chart composed of 18 colour fields and 6 greyscale fields. The spectral reflectance of each field was measured with a Konica Minolta KM2600d (Fig. 15).

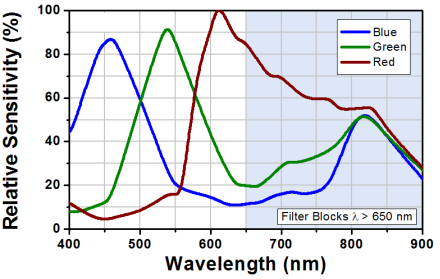


Fig. 14. An example of typical curves of spectral sensitivity of an RGB camera [47].

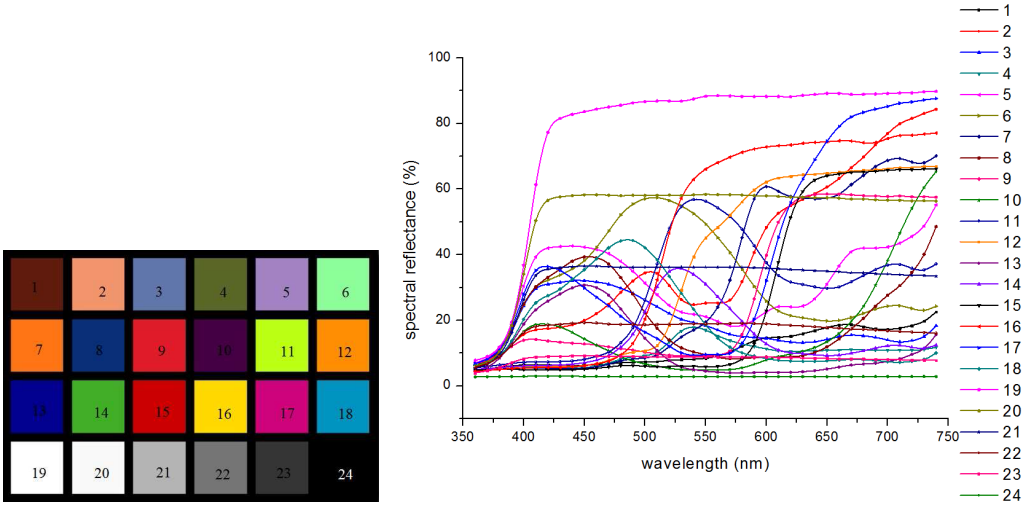


Fig. 15. A view of the Macbeth colour chart (on the left) and (on the right) spectral reflectance of the fields of the test (the numbers of the curves are correlated with the numbers of samples on the chart).

After illuminating the colour chart (at a distance of 100 mm – due to the required field of view of the camera) with white light with the assumed CCT, images of the chart were registered with an RGB micro-camera situated next to the output of homogenizing rod. Comparison of the results for each colour sample are presented in Fig. 16. The registered images depend on three factors: the spectral reflectance of the sample field, SPD of light used to illuminate the sample and the spectral sensitivity of the camera. Comparing the images of each field with the view of the sample test it can be stated that for imaging and good rendering of objects containing various colour components light with a matched CCT should be used, which shows an advantage of tuneable sources. The main reason of obtaining high quality lighting for an individual sample is correlation of the source SPD's shape and the spectral reflectance of the sample. However, samples 9 and 15 still seem to be rendered not properly. The reason of this situation is a decrease of the spectral sensitivity of the colour camera in the long wavelength region. In the case of a white sample the higher CCT the better rendering, but when SPD with the CCT of illuminant A is used it is impossible to distinguish between white (sample 19) and yellow (sample 16).

| Sample number | Test sample | Multi-emitter 2856 K | Multi-emitter 3500 K | Multi-emitter 4500 K | Multi-emitter 5500 K | Multi-emitter 6500 K | Best visual correlation |
|---|---|---|---|---|---|---|---|
| 1 | | | | | | | 4500 K |
| 2 | | | | | | | 4500 K |
| 3 | | | | | | | 5500 K |
| 4 | | | | | | | 5500 K |
| 5 | | | | | | | 5500 K |
| 6 | | | | | | | 5500 K |
| 7 | | | | | | | 2856 K |
| 8 | | | | | | | 4500 K |
| 9 | | | | | | | 5500 K |
| 10 | | | | | | | 5500 K |
| 11 | | | | | | | 6500 K |
| 12 | | | | | | | 2856 K |
| 13 | | | | | | | 4500 K |
| 14 | | | | | | | 5500 K |
| 15 | | | | | | | 5500 K |
| 16 | | | | | | | 5500 K |
| 17 | | | | | | | 5500 K |
| 18 | | | | | | | 6500 K |
| 19 | | | | | | | 6500 K |

Fig. 16. Views of each field of the colour chart under white light with various CCT.

If we compare the high CCT images of the colour chart obtained after illuminating it with PC LED (CCT = 6000 K) and multi-emitter white light (D55 and D65) (Fig. 17), a visual difference can be observed especially for samples including very short wavelengths (2, 3, 4, 5, 6, 8, 10, 11, 13 and 18). PC LED is also poorly rendering grey scale samples.

When comparing the images of the colour chart taken under illumination of PC LED (CCT = 3300 K) and multi-emitter white light (2856 K and 3500 K) (Fig. 18), the visual difference are not significant; small differences can be observed especially for samples: 6, 17 and 18. All low-CCT sources poorly render grey scale samples.

Fig. 17. Comparison of the image of the colour chart illuminated with: on the left – a multi-emitter source with CCT = 5500 K; in the middle – a phosphor-converting white LED with CCT = 6000 K; on the right – a multi-emitter source with CCT = 6500 K.

Fig. 18. Comparison of the image of the colour chart illuminated with: on the left – a multi-emitter source with CCT = 2856 K; in the middle – a phosphor-converting white LED with CCT = 3300 K; on the right – a multi-emitter source with CCT = 3500 K.

## 4. Conclusions

The aim of the research was to construct and analyse selected colorimetric properties of a multi-emitter tuneable source (correlated colour temperature, colour rendering, colour fidelity and distance from the Planckian locus). We obtained a LED-based source characterized by better colour rendering than the most popular sources – white PC-LEDs and *fluorescent lamps* (FLs) with capability of tuning. The difference is significant, especially for $R_9$ index. However, considering only the colour rendering index may be confusing. That is why we have analysed also *Duv* and $\Delta u'v'$. There are no similar constructions when we consider endoscopy; in other applications the authors do not characterize their systems in such detail. Additionally, only integrating spheres are used in such systems – we have excluded them and replaced by a homogenizing rod in order to obtain better energy efficiency. We proved that our source is more efficient in terms of visual performance in comparison with typical medical lamps. In order to do it we illuminated the Macbeth colour chart, where each field was characterized by different spectral reflectance. We proved that–depending on the shape of this characteristic–various SPDs should be used to obtain excellent visual performance (see last column in Fig. 16). Only a tuneable source can assure variability of SPD in a wide range of CCT and for this reason it exceeds the advantages of other light sources.

The results of our radiometric and colorimetric measurements and analysis confirm that it is possible to design and construct a high-quality source for application in endoscopes to illuminate

the working area with both white light characterized by very high rendering parameters and narrow-band radiation. The main advantage of using a tuneable source of white light is visible in Fig. 16 – for various colour samples SPD of the light source should be different and adapted to the spectral characteristics of the sample in order to recognize and properly distinguish colours of the object. It is extremely important when we take into account the endoscopic applications. Additionally, the multispectral technique could be applied to build a device enabling visual evaluation and analysis of the reflectance spectra of objects under narrow-band illumination, which enables to use it for constructing a PDT endoscope. Altogether, it creates the unique (for this moment) construction combining the possibility of observation inside of the objects in various applications with very good quality tuneable white light and the multispectral technique. It may also be used in the laboratory applications when this kind of light is required in experiments.

***Acknowledgements***

This paper was prepared on the basis of the results of the research framework S/WE/3/2018 obtained in the Department of Electric Power Engineering, Photonics and Lighting Technology, Bialystok University of Technology.

**References**

[1] Yeh, N., Ding, T.J., Yeh, P. (2015). Light-emitting diodes' light qualities and their corresponding scientific applications. *Renewable and Sustainable Energy Reviews*, 51, 55–61.

[2] Clancy, N.T., Li, R., Rogers, K., Driscoll, P., Excel, P., Yandle, R., Elson, D.S. (2012). Development and evaluation of a light-emitting diode endoscopic light source. *Proc. SPIE*, 8214, 82140R.

[3] Swain, P., Iddan, G.J., Meron, G., Glukhovsky, A. (2001). Wireless capsule endoscopy of the small bowel: development, testing, and first human trials. *Proc. SPIE*, 4158, 19–24.

[4] Jeng, W.D., Mang, O.Y., Chen, Y.T., Wu, Y.Y. (2011). Design of illumination system in ring field capsule endoscope. *Proc. SPIE*, 7893, 78930E.

[5] Lee, A.C., Elson, D.S., Neil, M.A., Kumar, S., Ling, B.W., Bello, F., Hanna, G.B. (2009). Solid-state semiconductors are better alternatives to arc-lamps for efficient and uniform illumination in minimal access surgery. *Surgical endoscopy*, 23(3), 518–526.

[6] Lu, M.K., Chang, F.C., Wang, W.Z., Hsieh, C.C., Kao, F.J. (2014). Compact light-emitting diode lighting ring for video-assisted thoracic surgery. *Journal of biomedical optics*, 19(10), 105004.

[7] Khan, T.Q., Bodrogi, P., Vinh, Q.T., Winkler, H. (Eds.). (2015). *LED lighting: Technology and perception*. John Wiley & Sons.

[8] Papamichael, K., Siminovitch, M., Veitch, J.A., Whitehead, L. (2016). High color rendering can enable better vision without requiring more power. *Leukos*, 12(1–2), 27–38.

[9] Bois, C., Bodrogi, P., Khanh, T. Q., Winkler, H. (2014). Measuring, simulating and optimizing current LED phosphor systems to enhance the visual quality of lighting. *Journal of Solid State Lighting*, 1(1), 5.

[10] Brown, S.W., Rice, J.P., Neira, J.E., Johnson, B.C., Jackson, J.D. (2006). Spectrally tunable sources for advanced radiometric applications. *Journal of research of the National Institute of Standards and Technology*, 111(5), 401.

[11] Burgos-Fernandez, F.J., Vilaseca, M., Perales, E., Herrera-Ramirez, J.A., Martínez-Verdú, F.M., Pujol, J. (2016). Spectrally tunable light source based on light-emitting diodes for custom lighting solutions. *Optica Applicata*, 46(1), 117–129.

[12] Hu, N.C., Wu, C.C., Chen, S.F., Hsiao, H.C. (2008). Implementing dynamic daylight spectra with light-emitting diodes. *Applied optics*, 47(19), 3423–3432.

[13] Wu, C.C., Hu, N.C., Fong, Y.C., Hsiao, H.C., Hsiao, S.L. (2012). Optimal pruning for selecting LEDs to synthesize tunable illumination spectra. *Lighting Research & Technology*, 44(4), 484–497.

[14] Blaszczak, U.J., Gryko, L., Zajac, A. (2017). Tunable white light source for medical applications. *Proc. SPIE*, 10445, 104453Y.

[15] Afshari, S., Mishra, S., Julius, A., Lizarralde, F., Wason, J.D., Wen, J.T. (2014). Modeling and control of color tunable lighting systems. *Energy and Buildings*, 68, 242–253.

[16] LeGendre, C., Yu, X., Debevec, P. (2017). Optimal LED selection for multispectral lighting reproduction. *Electronic Imaging*, (8), 25–32.

[17] Parmar, M., Lansel, S., Farrell, J. (2012). An LED-based lighting system for acquiring multispectral scenes. *Proc. SPIE*, 8299, 82990P.

[18] Wu, T., Lin, Y., Zheng, L., Guo, Z., Xu, J., Liang, S., Chen, Z. (2018). Analyses of multi-color plant-growth light sources in achieving maximum photosynthesis efficiencies with enhanced color qualities. *Optics express*, 26(4), 4135–4147.

[19] Oh, J.H., Yang, S.J., Do, Y.R. (2014). Healthy, natural, efficient and tunable lighting: four-package white LEDs for optimizing the circadian effect, color quality and vision performance. *Light: Science & Applications*, 3(2), e141.

[20] Blaszczak, U.J., Aziz, D.A., Gryko, L. (2017). Influence of the spectral composition of LED lighting system on plants cultivation in a darkroom. *Proc. SPIE*, 10445, 104453V.

[21] Haff, R.P., Pearson, T.C., Maghirang, E. (2013). A multispectral sorting device for isolating single wheat kernels with high protein content. *Journal of Food Measurement and Characterization*, 7(4), 149–157.

[22] Fu, X., Wang, X., Rao, X. (2017). An LED-based spectrally tuneable light source for visible and near-infrared spectroscopy analysis: A case study for sugar content estimation of citrus. *Biosystems Engineering*, 163, 87–93.

[23] Lin, D., Zhong, P., He, G. (2017). Color temperature tunable white LED cluster with color rendering index above 98. *IEEE Photonics Technology Letters*, 29(12), 1050–1053.

[24] Molada Tebar, A., Lerma, J.L., Marqués Mateu, Á. (2018). Camera characterization for improving color archaeological documentation. *Color Research & Application*, 43(1), 47–57.

[25] ul Rehman, A., Anwer, A.G., Goldys, E.M. (2017). Programmable LED-based integrating sphere light source for wide-field fluorescence microscopy. *Photodiagnosis and photodynamic therapy*, 20, 201–206.

[26] Bartczak, P., Gebejes, A., Fält, P., Hauta-Kasari, M. (2016). An LED-based tunable illumination for diverse medical applications. *Computer-Based Medical Systems (CBMS)*, 2016 IEEE 29th International Symposium, 292–293.

[27] Dubey, V., Singh, G., Singh, V., Ahmad, A., Mehta, D. S. (2016). Multispectral quantitative phase imaging of human red blood cells using inexpensive narrowband multicolor LEDs. *Applied optics*, 55(10), 2521–2525.

[28] Herrera-Ramírez, J., Vilaseca, M., Pujol, J. (2014). Portable multispectral imaging system based on light-emitting diodes for spectral recovery from 370 to 1630 nm. *Applied optics*, 53(14), 3131–3141.

[29] Rubins, U., Spigulis, J., Valeine, L., Berzina, A. (2013). Semi-automatic detection of skin malformations by analysis of spectral images. *Proc. OSA*, 8798, 87980.

[30] Delpueyo, X., Vilaseca, M., Royo, S., Ares, M., Rey-Barroso, L., Sanabria, F., Solomita, G. (2017). Multispectral imaging system based on light-emitting diodes for the detection of melanomas and basal cell carcinomas: a pilot study. *Journal of biomedical optics*, 22(6), 065006.

[31] Blaszczak, U., Gilewski, M., Gryko, L., Zajac, A., Kukwa, A., Kukwa, W. (May 2014). Applications of optical fibers and miniature photonic elements in medical diagnostics. *Proc. SPIE*, 9228, 92280J.

[32] American National Standard for Electric Lamps – Specifications for the Chromaticity of Solid State Lighting (SSL) Products ANSI, C78.377-2017.1

[33] Van Driel, W.D., Fan, X., Zhang, G.Q. (eds.). (2017). *Solid State Lighting Reliability Part 2: Components to Systems*, 3, Springer.

[34] Shen, J., Chang, S., Wang, H., Zheng, Z. (2017). Optimising the illumination spectrum for enhancing tissue visualisation. *Lighting Research & Technology*, 1477153517732812.

[35] Wang, H.C., Chen, Y.T. (2012). Optimal lighting of RGB LEDs for oral cavity detection. *Optics express*, 20(9), 10186–10199.

[36] Lee, M.H., Seo, D.K., Seo, B.K., Park, J.I. (2009). Optimal illumination for discriminating objects with different spectra. *Optics letters*, 34(17), 2664–2666.

[37] Shen, J., Chang, S., Wang, H., Zheng, Z. (2016). Optimal illumination for visual enhancement based on color entropy evaluation. *Optics express*, 24(17), 19788–19800.

[38] CIE224:2017. *Colour Fidelity Index For Accurate Scientific Use.*

[39] Standard PN-EN 60601-2-41: 2010 / A1: 2015-09E – Medical electrical equipment – Part 2-41: Particular requirements for the basic safety and essential performance of surgical luminaires and luminaires for diagnosis, (2015).

[40] Gryko, L., Zajac, A., Szymanska, J., Blaszczak, U., Palkowska, A., Kulesza, E. (2016). Semiconductor lasers vs LEDs in diagnostic and therapeutic medicine. *Proc. SPIE*, 10159, 101590I.

[41] Gryko, L., Blaszczak, U., Zajac, A., Palkowska, A. (2016). Evaluation of possibility of correlated color temperature modelling for high power LEDs set. *Przeglad Elektrotechniczny*, 92(9), 157–162.

[42] Błaszczak, U., Gilewski, M., Gryko, Ł., Zając, A. (2016). Investigation of the supply influence to chosen optical parameters of the LEDs set. *Przegląd Elektrotechniczny*, 92(9), 150–153.

[43] Gilewski, M., Gryko, L., Zajac, A. (2013). Digital controlling system to the set of high power LEDs. *Proc. SPIE*, 8902, 89021D.

[44] Gilewski, M. (2010). Multi-channel, DC current supply system for set of high power LED. *Przeglad Elektrotechniczny*, 86(10), 193–196.

[45] Gryko, L., Blaszczak, U.J., Zajac, A.S. (2018). Colorimetric characterization of the tunable LED-based light source at the output of the homogenizing rod. *Proc. SPIE*, 10808, 1080811.

[46] Blaszczak, U.J., Gryko, L., Palkowska, A., Kulesza, E., Zajac, A. (2016). Color mixing in LED illuminating system for endoscopic purposes. *IEEE*, 1–6.

[47] Product CCD & CMOS Cameras. *http://www.thorlabs.com* (Jun. 2018).